Available online at www.sciencedirect.com
SCIENCE DIRECT
Journal of Physics and Chemistry of Solids 67 (2006) 336–339
JOURNAL OF PHYSICS AND CHEMISTRY OF SOLIDS
www.elsevier.com/locate/jpcs

Resonant enhancement of electronic Raman scattering

A.M. Shvaika [a,*], O. Vorobyov [a], J.K. Freericks [b], T.P. Devereaux [c]

[a] Institute for Condensed Matter Physics of the National Academy of Sciences of Ukraine, 1 Svientsitskii Street, 79011 Lviv, Ukraine
[b] Department of Physics, Georgetown University, Washington, DC 20057, USA
[c] Department of Physics, University of Waterloo, Ont., Canada N2L 3GI

Abstract

We present an exact solution for electronic Raman scattering in a single-band, strongly correlated material, including nonresonant, resonant and mixed contributions. Results are derived for the spinless Falicov–Kimball model, employing dynamical mean field theory; here, we focus on the Mott insulator phase.

Electronic Raman scattering is an important probe of the electronic excitations in materials. It has been used to examine different kinds of charge and spin excitations in a variety of different materials, ranging from Kondo insulators [1,2], to high temperature superconductors [3,4], to ruthenium oxide materials [5]. Inelastic light scattering involves contributions from scattering processes that depend on the incident photon frequency (so-called mixed and resonant contributions) and processes that are independent of the incident photon frequency (so-called nonresonant contributions). There has been much theoretical work on this problem. In the strong-coupling regime, a perturbative approach has been used, and has illustrated a number of important features of resonant scattering processes [6,7]. The nonresonant case has also been examined, and an exact solution for correlated systems (in large spatial dimensions) is available for both the Falicov–Kimball [8] and Hubbard [9] models. Here we concentrate on an exact solution of the full problem for the Falicov–Kimball model including all resonant and mixed effects.

The Falicov–Kimball model Hamiltonian [10] is (at half filling)

$$\mathcal{H} = -\frac{t^*}{\sqrt{d}} \sum_{\langle ij \rangle} c_i^\dagger c_j + U \sum_i \left(c_i^\dagger c_i - \frac{1}{2} \right) \left(w_i - \frac{1}{2} \right) \tag{1}$$

and includes two kinds of particles: conduction electrons, which are mobile, and localized electrons which are immobile. Here $c_i^\dagger$ (c_i) creates (destroys) a conduction electron at site i, w_i is the localized electron number at site i, U is the on-site Coulomb interaction between the electrons, and t^* is the hopping integral (which we use as our energy unit). The symbol d is the spatial dimension, and ij denotes a sum over all nearest neighbor pairs (we work on a hypercubic lattice). The model is exactly solvable with dynamical mean field theory when $d \to \infty$ [11,12] (see [13] for a review).

Shastry and Shraiman [6] derived an explicit formula for inelastic light scattering that involves the matrix elements of the electronic vector potential for light with the many-body states of the correlated system. Their expression for the Raman response (in a Lehmann representation) is

$$R(\Omega) = 2\pi \sum_{i,f} \exp(-\beta \varepsilon_i) \delta(\varepsilon_f - \varepsilon_i - \Omega) \times \left| \frac{hc^2}{V\sqrt{\omega_i \omega_o}} e_\alpha^i e_\beta^o \langle f | \hat{M}^{\alpha\beta} | i \rangle \right|^2 / \mathcal{Z} \tag{2}$$

for the scattering of electrons by optical photons (the repeated indices α and β are summed over). Here, $\varepsilon_{i(f)}$ refers to the energies of the initial (final) eigenstates describing the 'electronic matter', $\mathcal{Z}$ is the partition function, and

$$\langle f | \hat{M}^{\alpha\beta} | i \rangle = \langle f | \gamma_{\alpha,\beta} | i \rangle + \sum_l \left(\frac{\langle f | j_\beta | l \rangle \langle l | j_\alpha | i \rangle}{\varepsilon_l - \varepsilon_i - \omega_i} + \frac{\langle f | j_\alpha | l \rangle \langle l | j_\beta | i \rangle}{\varepsilon_l - \varepsilon_i + \omega_o} \right) \tag{3}$$

is the scattering operator constructed by the current $j_\alpha = \sum_{\mathbf{k}} \partial \varepsilon(\mathbf{k}) / \partial k_\alpha c_{\mathbf{k}}^\dagger c_{\mathbf{k}}$, and stress-tensor $\gamma_{\alpha\beta} = \sum_{\mathbf{k}} \partial^2 \varepsilon(\mathbf{k}) / \partial k_\alpha \partial k_\beta c_{\mathbf{k}}^\dagger c_{\mathbf{k}}$ operators, with $\varepsilon(\mathbf{k})$ the band structure and $c_{\mathbf{k}}$ the destruction operator for an electron with momentum $\mathbf{k}$. Since the scattering operator enters to the second power in the Raman response, there are three kinds of terms in the response

* Corresponding author. Tel.: +380 322 761054; fax: +380 322 761158.
E-mail address: ashv@icmp.lviv.ua (A.M. Shvaika).

0022-3697/$ - see front matter © 2005 Elsevier Ltd. All rights reserved.
doi:10.1016/j.jpcs.2005.10.048

function: the $\gamma\gamma$ term gives the nonresonant response, the γj term gives the mixed response, and the jj terms give the resonant response.

We use a diagrammatic technique to exactly determine all of the contributions to the Raman response function $\chi(\Omega)$

$$R(\Omega) = \frac{2\pi h^2 c^4}{V^2 \omega_i \omega_o} \frac{\chi(\Omega)}{1-\exp(-\beta\Omega)}, \tag{4}$$

which is the result directly measured by experimentalists. We explicitly present results for the Stokes Raman response (the electrons absorb energy from the photon during the scattering), with an incident photon frequency ω_i, an outgoing photon frequency ω_o, and a transfered photon frequency $\Omega = \omega_i - \omega_o$. The procedure is complicated, and involves first computing the response functions on the imaginary time axis, then Fourier transforming to imaginary frequencies, and finally performing an analytic continuation to the real axis; the relevant formulas, and a summary of the techniques are presented elsewhere [14].

We analyze three different symmetries for the electronic charge excitations that scatter the light. The A_{1g} symmetry has the full symmetry of the lattice and is measured by taking the initial and final photon polarizations to be $\mathbf{e}^i = \mathbf{e}^o = (1,1,1,\ldots)$. The B_{1g} symmetry is a d-wave-like symmetry that involves crossed polarizers: $\mathbf{e}^i = (1,1,1,\ldots)$ and $\mathbf{e}^o = (-1,1,-1,1,\ldots)$. Finally, the B_{2g} symmetry is another d-wave symmetry rotated by 45 degrees; with $\mathbf{e}^i = (1,0,1,0,\ldots)$ and $\mathbf{e}^o = (0,1,0,1,\ldots)$.

It turns out that the A_{1g} sector has contributions from nonresonant, mixed, and resonant Raman scattering, the B_{1g} sector has contributions from nonresonant and resonant Raman scattering only, and the B_{2g} sector is purely resonant [8]. Since the end result is so complex, we first examine the bare response function (which has no contributions from vertex corrections) because it yields some interesting insights. All the bare diagrams can be summed up and rewritten in the following form

$$\chi_{\text{bare}}(\Omega) = \frac{1}{N}\sum_{\mathbf{k}} \int_{-\infty}^{+\infty} d\omega [f(\omega) - f(\omega+\Omega)] A_{\mathbf{k}}(\omega) A_{\mathbf{k}}(\omega+\Omega) \times |\gamma_{\mathbf{k}} + v^i_{\mathbf{k}} v^o_{\mathbf{k}} [G_{\mathbf{k}}(\omega+\omega_i+i\delta) + G_{\mathbf{k}}(\omega-\omega_o-i\delta)]|^2, \tag{5}$$

where $\gamma_{\mathbf{k}} = \sum_{\alpha,\beta} e^i_\alpha \partial\varepsilon(\vec{k})/\partial k_\alpha \partial k_\beta e^o_\beta$, $v^{i,o}_{\mathbf{k}} = \sum_\alpha e^{i,o}_\alpha \partial\varepsilon(\vec{k})/\partial k_\alpha$, $A_{\mathbf{k}}(\omega) = -(1/\pi)\text{Im}G_{\mathbf{k}}(\omega - i\delta)$, $G_{\mathbf{k}}(\omega)$ is the momentum-dependent single-electron Green's function, and $f(\omega) = 1/[1+\exp(\beta\omega)]$ is the Fermi distribution function.

In general, the bare response function in Eq. (5) is a function of the frequency shift, the incoming photon frequency and the outgoing photon frequency; it is enhanced when one or both of the denominators of the Green's functions of the expression on the last line are resonant (i.e. approaches zero). Then we have a so-called 'double' or 'multiple resonance' [15]. The full response function also includes vertex renormalizations. But since the total (reducible) charge vertex for the Falicov–Kimball model does not diverge by itself, then it does not introduce any additional vanishing energy denominators or 'resonances'; it only leads to a mild renormalization of the total Raman response.

The Falicov–Kimball model on a $d = \infty$ hypercubic lattice has a Mott transition into a pseudogap-like phase at half filling when $U = \sqrt{2}$. We examine the system on the insulating side of the Mott transition at $U = 3$. Our results for the total Raman response as a function of the transfered frequency Ω for different temperatures appear in Fig. 1 for the incident photon frequencies $\omega_i = 2.5$ and ∞, and in Fig. 2 for $\omega_i = 2$.

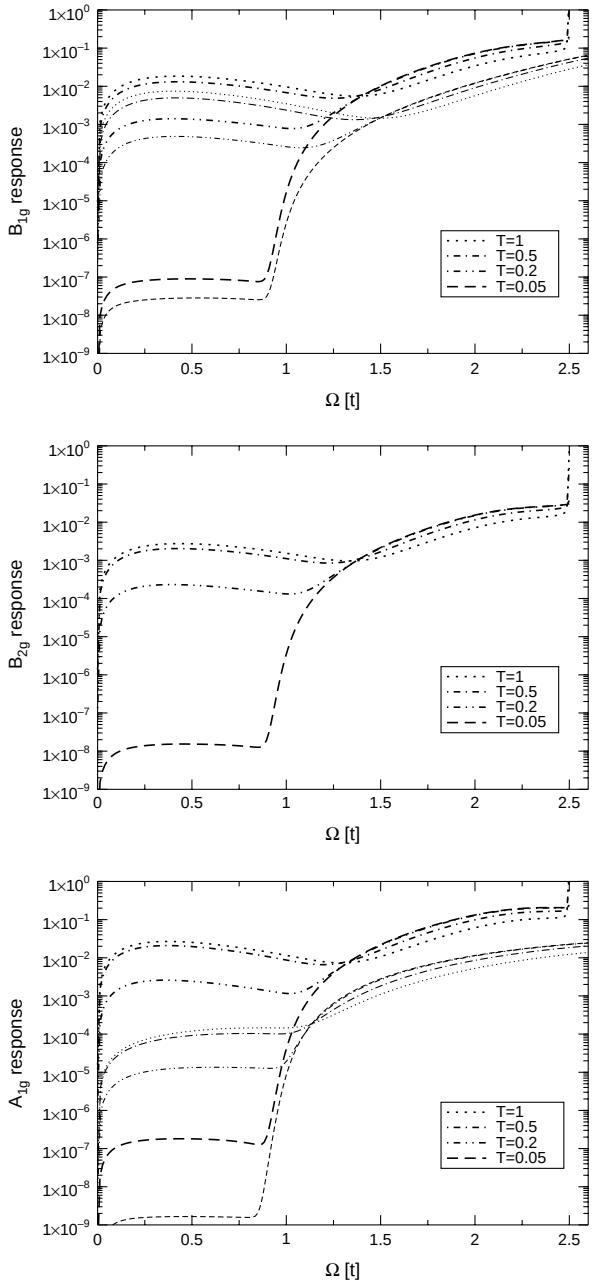

Fig. 1. Isosbestic behavior of the resonant Raman response for $U = 3$ and $\omega_i = 2.5$ (thick lines) and $\omega_i = \infty$ (nonresonant response, thin lines). Different lines correspond to different temperatures $T = 1, 0.5, 0.2, 0.05$. Note that the $\omega_i = 2.5$ curves all cross at two isosbestic points: one close to $U/2$ and another close to ω_i.

For the $\omega_i = \infty$ case (thin lines in Fig. 1) we have a pure nonresonant response that is nonzero only in the A_{1g} and B_{1g} channels. One can see, that in both channels all lines, which correspond to different temperatures, cross at a characteristic frequency $\Omega \approx U/2$ (isosbestic point) where the Raman response is independent of temperature. In Ref. [8], isosbestic behavior was observed for the nonresonant response only in the B_{1g} channel, but in Fig. 1 it is also seen in the A_{1g} channel when the response is plotted on a logarithmic scale. When the incident photon frequency decreases (thick lines in Fig. 1), we also have a nonzero Raman response in the B_{2g} channel and the shape of the Raman response is changed. In particular, a sharp peak appears at the double resonance located at $\Omega = \omega_i$, and the full response is not just an enhancement of the nonresonant features (which are apparent when the incident photon frequency becomes large), but the shape of the response can change dramatically due to resonant effects. This is most apparent when the incident photon energy is close to U. Also, the initial $\omega_i = \infty$ isosbestic point is shifted and a second isosbestic point appears in the double resonance area of $\Omega \approx \omega_i$. With a further decrease of the incident photon frequency, both isosbestic points approach one another (Fig. 2) and then disappear when $\omega_i \approx U/2$.

In Fig. 3, we plot the resonant profile for the Raman response at various (fixed) transfered frequencies Ω as a function of the incident photon frequency ω_i. Note that when Ω is larger than the energy of the charge-transfer excitation ($\Omega > U$) we only

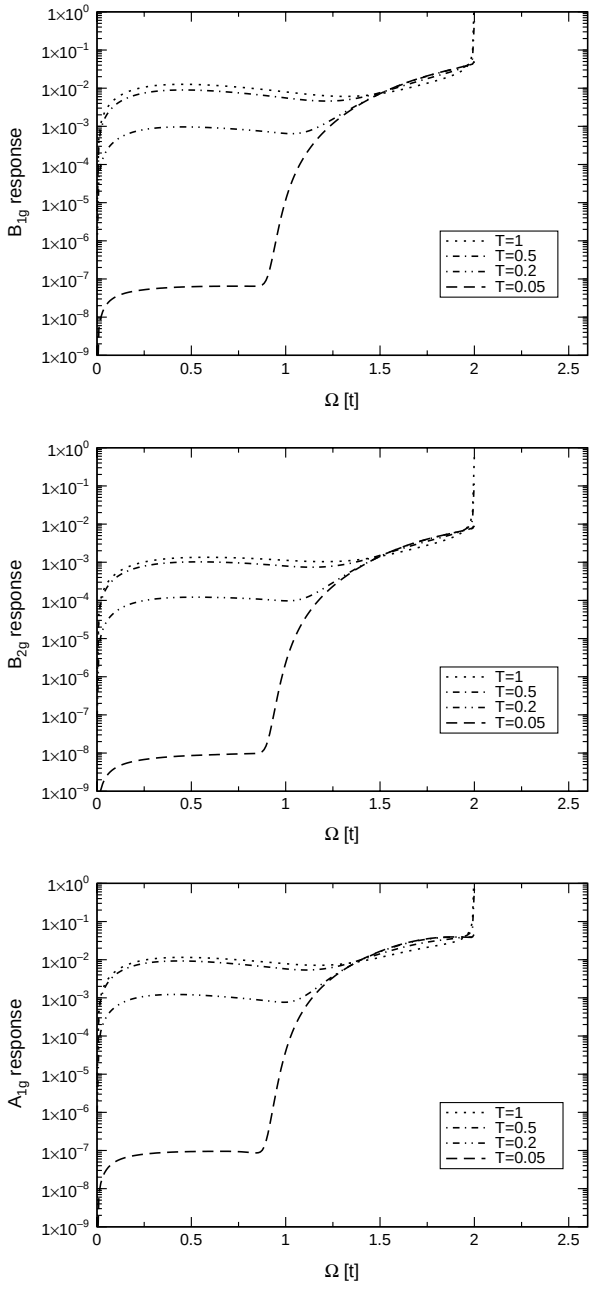

Fig. 2. The same plot as in Fig. 1, but for the case $\omega_i = 2$.

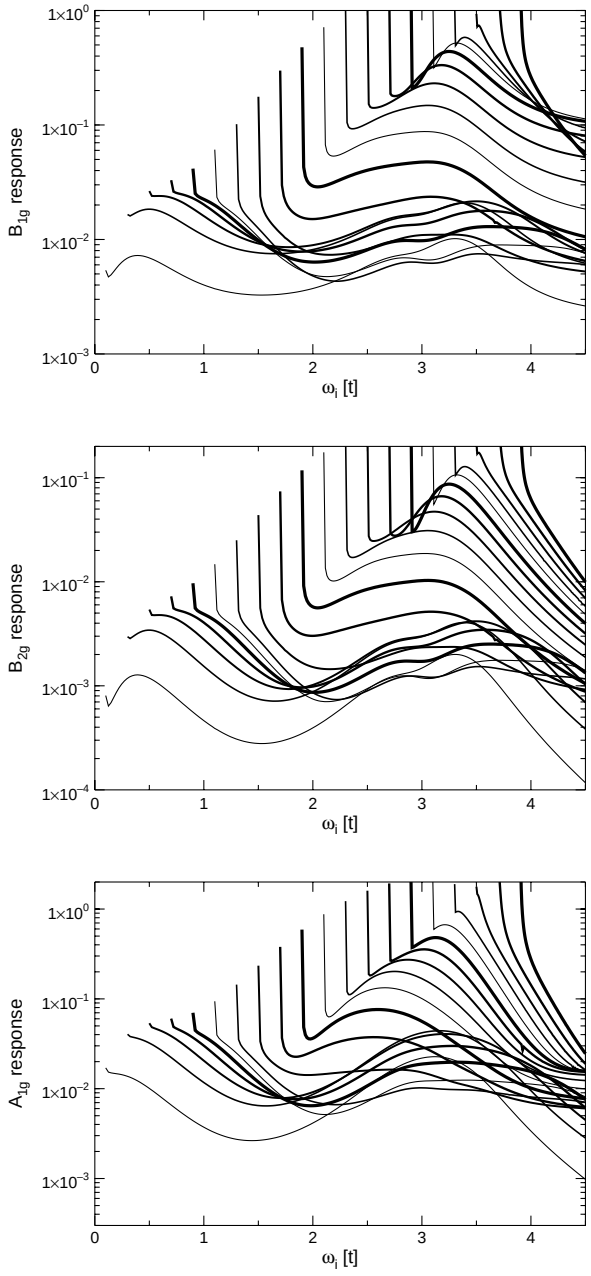

Fig. 3. Raman response at various values of the transfered frequency Ω in steps of 0.2 as a function of the incident photon frequency ω_i for $T = 0.5$. All curves start at $\omega_i = \Omega$.

observe the double resonance at $\Omega_i = \omega$ and there are no additional features in the resonant profile. When Ω decreases and moves into the charge-transfer peak region, a resonant enhancement of the charge-transfer peak at $\omega_i \approx U$ is observed. Its location and width change with a further decrease of the transfered frequency and it almost disappears when Ω lies between the charge-transfer and low-energy peaks, and is then restored when Ω moves into the low-energy peak region, where it has a double-peak structure for the B_{1g} and B_{2g} channels. So, we observe a joint resonance of the charge-transfer and low-energy peaks, and this resonance of a low-energy feature due to a higher-energy photon has been seen in the Raman scattering of some strongly correlated materials [3,4] (the low-energy spin-wave resonance in the high-temperature superconductors displays this qualitative behavior, since it shows strong resonant effects at a transfered energy that is almost an order of magnitude smaller than the incident photon energy).

In conclusion, we have performed an exact calculation of the electronic Raman response function for a strongly correlated system in the insulating phase and described three interesting resonant features: (1) the appearance of a double-resonance peak when the transfered energy approaches the incident photon energy, (2) the appearance of two isosbestic points in all symmetry channels, and (3) a joint resonance of the charge transfer and low energy peaks when the incident photon frequency is on the order of U. It will be interesting to see whether these features can be seen in future experiments on correlated systems.

Acknowledgements

We acknowledge support from the US Civilian Research and Development Foundation (CRDF Grant No. UP2-2436-LV-02). J.K.F. also acknowledges support from the National Science Foundation under Grant No. DMR-0210717. T.P.D. acknowledges the NSERC, PREA and the Alexander von Humboldt foundation for support.

References

[1] P. Nyhus, S.L. Cooper, Z. Fisk, Phys. Rev. B 51 (1995) 15626.
[2] P. Nyhus, S.L. Cooper, Z. Fisk, J. Sarrao, Phys. Rev. B 52 (1995) R14308 (Phys. Rev. B 55 (1997) 12488).
[3] K.B. Lyons, P.A. Fleury, L.F. Schneemeyer, J.V. Waszczak, Phys. Rev. Lett. 60 (1988) 732; S. Sugai, S. Shamoto, M. Sato, Phys. Rev. B 38 (1988) 6436; P.E. Sulewsky, P.A. Fleury, K.B. Lyons, S.-W. Cheong, Z. Fisk, Phys. Rev. B 41 (1990) 225; R. Liu, M.V. Klein, D. Salamon, S.L. Cooper, W.C. Lee, S.-W. Cheong, D.M. Ginsberg, J. Phys. Chem. Solids 54 (1993) 1347.
[4] G. Blumberg, P. Abbamonte, M.V. Klein, W.C. Lee, D.M. Ginsberg, L.L. Miller, A. Zibold, Phys. Rev. B 53 (1996) 11930.
[5] H.L. Liu, S. Yoon, S.L. Cooper, G. Cao, J.E. Crow, Phys. Rev. B 60 (1999) R6980.
[6] B.S. Shastry, B.I. Shraiman, Phys. Rev. Lett. 65 (1990) 1068 (Int. J. Mod. Phys. B 5 (1991) 365).
[7] A.V. Chubukov, D.M. Frenkel, Phys. Rev. B 52 (1995) 9760 (Phys. Rev. Lett. 74 (1995) 3057); D.K. Morr, A.V. Chubukov, Phys. Rev. B 56 (1997) 9134.
[8] J.K. Freericks, T.P. Devereaux, Condens. Matter Phys. 4 (2001) 149 (Phys. Rev. B 64 (2001) 125110).
[9] J.K. Freericks, T.P. Devereaux, R. Bulla, Phys. Rev. B 64 (2001) 233114; J.K. Freericks, T.P. Devereaux, R. Bulla, Th. Pruschke, Phys. Rev. B 67 (2003) 155102.
[10] L.M. Falicov, J.C. Kimball, Phys. Rev. Lett. 22 (1969) 997.
[11] W. Metzner, D. Vollhardt, Phys. Rev. Lett. 62 (1989) 324.
[12] U. Brandt, C. Mielsch, Z. Phys. B: Condens. Matter 75 (1989) 365 (79 (1990) 295; 82 (1991) 37).
[13] J.K. Freericks, V. Zlatić, Rev. Mod. Phys. 75 (2003) 1333.
[14] A.M. Shvaika, O. Vorobyov, J.K. Freericks, T.P. Devereaux, Phys. Rev. Lett 93 (2004) 137402 (Phys. Rev. B 71 (2005) 045120).
[15] R.M. Martin, L.M. Falicov, in: M. Cardona (Ed.), Light Scattering in Solids, Springer, New York, 1975.